Chapter 1

Long baseline observations with LOFAR

Observations using international LOFAR baselines have obtained science quality images with resolution $0.3''$ and rms noise $0.15\,\mathrm{mJy\,beam^{-1}}$ at 154 MHz, see for example [2]. In this chapter we will describe the similarities and differences in the observations and subsequent processing as compared to LOFAR imaging using shorter (NL) baselines. This chapter is meant to serve as a reference for you who want to plan observations or calibrate and image LOFAR data using the longest LOFAR baselines. [1] In section 1.1 we give a brief theoretical background and introduce concepts and vocabulary relevant for long baseline LOFAR observations. In the following section 1.2 we list practical commands, examples and code refereces to assist in your calibration and imaging of LOFAR data. In section 1.3 we summarise the most important points to remember when scheduling long baseline observations. Please note that in this chapter, the term *long* baselines refers to international LOFAR baselines (i.e. length 1000 km) unless stated otherwise. We often use the term NL-LOFAR to refer to baselines including remote stations within the Netherlands, i.e. baselines of lengths <121 km.

1.1 Long baseline interferometry

The prime reason to use long baselines is to obtain very high-resolution images. Using the longest LOFAR baselines, subarcsecond imaging is possible in the HBA band and the upper part of the LBA band, see Table 1.1. However, the wide separation of stations means that each station sees a (very) different atmosphere, which means that visibility phases are generally less well behaved than on shorter baselines looking through a more similar patch of the atmosphere. Further more, the international stations cannot share the same clock (as the core stations do) and any offsets and drifts of the clocks will introduce delay errors between the stations. Finally, effects of visibility averaging are more prominent on long baselines, meaning that interference effects from strong sources in the field (e.g. Cas. A etc.) are greatly reduced thereby simplifying calibration. Because of these differences, a somewhat different calibration strategy is usually employed when imaging long baseline data than what is commonly used for LOFAR observations with shorter baselines. This need is nothing fundamentally new for LOFAR,

[1] The authors of this chapter are Eskil Varenius (`eskil.varenius@chalmers.se`) and Javier Moldon (`moldon@astron.nl`) with many useful contributions from the Long baselines working group.

in fact we may borrow many tools and knowledge developed for decades for use in very long baseline interferometry (VLBI) at centimeter wavelengths.

1.1.1 What do we want to image?

NL-LOFAR observations often aim to image a large area on the sky with moderate resolution for survey purposes as in the MSSS. In this case we usually want to make a single large (a degree or more) image. This is tricky for a number of reasons, as will be touched upon in more detail below, and is, in fact, the challenges which the major part of this cookbook revolves around. In such a large image, the sky is crowded with emission from different things, and accurate models of the brightest objects (and in particular the strongest sources like Cas. A) are required to make random noise limited images. However, on longer baselines the situation is different for a number of reasons. To begin with, we often want to image a particular object (e.g. M82) in great detail, and this object only subtends a very small (arcminute) part of the sky. Furthermore, at international baselines we are sensitive only to very compact emission. Many bright sources are partly resolved already at NL baselines, and not much flux density is actually present at international baselines, meaning that the sky is less crowded and the interferring sources are weaker. Finally, since we are interested in one (or many) small fields, we may average the data, thereby reducing interference from distant sources as well as reducing the computation required to calibrate and image the data. All in all, long baselines are in some ways easier to calibrate and image than NL-LOFAR!

1.1.2 Field of view: same, same but different

The area possible to image in a single LOFAR observation (NL or international) is limited by several factors such as:

- The station beam, i.e. the electric field response of a single LOFAR station limiting the signal to noise ratio far away from the pointing center. Although the flux densities of an image can be corrected using a good beam model, the lack of sensitivity will then manifest as larger rms image noise far from the phase center. Fundamentally speaking, the decrease in sensitivity cannot be corrected for, so if your source is weak and far from the phase center, you may have to re-observe with another pointing to see it. This effect is independent of baseline length, however: for long baselines we use international stations which are bigger than NL-remote stations, meaning a slightly smaller station beam with FWHM 1-2 degrees at HBA frequencies, see Table. 1.1.

- Geometrical/projection effects, such as W-projection artefacts. These can be corrected for in the imaging process using the AW-imager when making wide field images. This effect is more serious with long baselines, although fundamentally the same. However, since we are usually interested in small-field imaging, we may re-project the visibilites to another phase-center before imaging, decoupling the expensive projection process from the imaging.

- Variations in the atmosphere within the image. If the atmosphere is significantly non-uniform over your sky region of interest, you may need to use multi-directional calibration algorithms, e.g. SAGECAL, to calibrate your data. This can in principle be done, provided you have enough bright sources to serve as calibrators in your image, but may be computationally expensive. For long baselines, we are typically interested in only a few directions, reducing the computational demands.

- Averaging of visibility data, also referred to as time and frequency *smearing*. This effect reduces the amplitude of sources far from the phase center and may also distort the shape (typically enlarge them). As for the projection losses, averaging losses are more prominent at longer baselines. Here we need to take care during the observations, and subsequent initial processing, but if we do we can actually use the averaging effects to great advantage. By averaging, we reduce the impact of interferring sources, and reduce the data volume, thereby speeding up calibration and imaging.

- Disturbance from bright sources in the sky, e.g. Cas. A and others in the *A-team*. Interferring sources can be removed from the data provided you have a (very) good model of the soure, through *demixing* or similar procedures offered by the observatory. Interference from bright source may severely affect your dynamic range even if they are far away from the main beam of the station. This effect is actually much, much less of a problem on long baselines because we may average the data to greatly limit the field of view around the objec(s) we are interested in.

Generally, all the effects above need to be corrected for to some extent to make wide field images. But, when we are interested in one (or many) smaller parts of the sky and we have long baselines, we can focus on making several small-field images. Here we can use averaging to our advantage. By averaging the data, interference from distant (e.g. tens of arcminutes, depend on how much we average) sources is greatly reduced and calibration and imaging is thus simplified. However, some care is needed with averaging and therefore we elaborate a bit more on this concept below.

Time- and frequency smearing limiting field of view

Since correlators output a discrete set of visibilities (i.e. samples in time and frequency), averaging is to some extent always done on interferometric data. We may also average the data further after correlation to reduce the computational resources needed for calibration and imaging. Any averaging must however be done with care. Averaging a range of samples in time and frequency together corresponds to averaging over a small parallelogram in Fourier space. This means some information is lost, and one has to take care to not lose information that could affect the scientific results. For LOFAR, the standard *raw* data are delivered from the correlator with resolution 1 second in time, and 64/channels per subband. Each subband (using the standard 200 MHz clock) is 195 kHz wide, meaning that the limiting averaging bandwidth is 195/64kHz. This will limit the dynamic range at some distance from the observed phase center, similar to the station beam effects described above. A detailed description of the averaging losses is beyond the scope of this chapter, we merely quote the often used results by Bridle & Schwabb, see [1] chapter 18, who derived two expressions to estimate the average amplitude loss due to averaging in frequency and time, at some distance from the phase center. For frequency smearing, we can use their expression 18-24 assuming a square bandpass and circular Gaussian tapering, where the reduction in amplitude can be estimated as

$$\frac{I}{I_0} = \frac{\sqrt{\pi}}{2\sqrt{\ln 2}} \frac{\theta \nu_c}{r \Delta\nu} \mathrm{erf}\left(\sqrt{\ln 2} \frac{r \Delta\nu}{\theta \nu_c}\right) \tag{1.1}$$

where θ is the synthesized beam size (FWHM), ν_c is the central frequency of the observation, r is the distance from the phase center, and $\Delta\nu$ is the bandwidth. Note that the units of θ and r cancel if they are given in the same unit. Note also that this expression is in fact independent of central frequency ν_c since the synthesised beam also scales with ν_c, only the bandwidth is important.

For time smearing, we may use their formula 18-43, assuming a 12 hour average over a circular UV-coverage with Gaussian tapering:

$$\frac{I}{I_0} = 1 - 1.22 \times 10^{-9} \left(\frac{r}{\theta}\right)^2 \tau_a^2 \tag{1.2}$$

where τ_a is the averaging time in seconds.

What loss to define as acceptable of course depends on your science, in particular the brightness of your target, but as a general guide one may tolerate 5% loss in amplitude due to averaging. Using the standard LOFAR raw data values, we have calculated the corresponding circle (diameter, to compare with station FWHM) for different observing frequencies, see Table 1.1. We note that, except for the lowest LBA frequencies, we are limited by time averaging, where the 5% loss diameter is smaller than the station beam. Note that this limitation is not present for shorter baselines, and usually not a cause for worry in NL-LOFAR observations. But, with the longest baselines, the main restriction may (if you need excellent sensitivity) be the averaging by the raw data.

Freq. (MHz)	λ (m)	Int. PSF FWHM ($''$)	Int. station FHWM (deg)	5% loss, 1s Diam. (deg)	5% loss, 64ch/SB Diam. (deg)
15	19.99	3.30	19.39	11.73	4.29
30	9.99	1.65	9.70	5.86	4.29
45	6.66	1.10	6.46	3.91	4.29
60	5.00	0.82	4.85	2.93	4.29
75	4.00	0.66	3.88	2.35	4.29
120	2.50	0.41	2.59	1.47	4.29
150	2.00	0.33	2.07	1.17	4.29
180	1.67	0.27	1.73	0.98	4.29
200	1.50	0.25	1.55	0.88	4.29
210	1.43	0.24	1.48	0.84	4.29
240	1.25	0.21	1.29	0.73	4.29

Table 1.1: Station FWHM Values taken from [3, App. B]. Loss due to time- and frequency averaging as calculated using eqns. 1.2 and 1.1. Note that the expression given for frequency smearing is in fact independent of central frequency since the synthesised beam also scales with frequency, only the bandwidth is important.

1.1.3 The *shift + average* procedure

If we are interested in a single source, like the core of M82 which extends about 1 arcminute on the sky, we may average much more. For example, in the case of M82 the data were averaged to 1ch/SB and 10s meaning about 0.5% loss in amplitude at $30''$ from the phase center (thereby giving a FoV of 1 arcminute). Note however that when averaging this heavily in frequency or time, it is important to first check if there are large residual rates or delays in the data. If one is interested in multiple objects within the station beam, on needs to phase-shift (and re-project) the UV-data to each object before averaging. If M82 was not in the center of my field, but say $3'$ from the phase center, and I averaged as heavily as above without shifting first, I would decrease the amplitude of M82 with about 14%. The need for imaging multiple objects within the same primary beam has shown to be common enough for the Radio Observatory to implement this in the official pipelines. Starting during cycle three, you will

be able to request shifting and averaging of data to multiple phase centers within a beam as a part of your observation.

1.1.4 Calibration of international LOFAR stations

Data on long baselines are fundamentally no different from data on short baselines: calibration means to correct any errors in the visibility amplitudes and phases which were not included in the model applied when the data were correlated (such as atmospheric effects). If your target is very bright, you may be able to calibrate your data using the target itself. However, to find amplitude and phase corrections for the international stations, the target must be sufficiently bright on the angular scales measured by the baselines to the international stations. Because of the high resolution, calibration needs to be done using either a very compact source so that a point source model is good enough, or we need a very detailed model of the source structure. A science target is usually both weak and potentially has complex structure (on subarcsecond scales), which makes it hard to use for calibration of the international stations. Therefore, a nearby bright (and preferably compact) sources is usually observed along with the target.

The amplitude and phase errors are derived using the calibrator, and the corrections are then applied to the target before imaging. This is called phase-referencing, and in ordinary VLBI observations it is usually done by switching back and forth between target and calibrator since an ordinary dish can only point in a single direction at once. For ordinary VLBI observations this requires switching often enough so that the corrections derived for the calibrator is valid also when observing the target source, but since LOFAR provides multiple beams, we may observe the calibrator and target simultaneously, simplifying calibration compared to ordinary VLBI.

However, the calibrator must also be close enough to the target for the corrections derived to be valid also in the direction of the target. Preliminary investigations indicate that the separation between calibrator and target should not be larger than 5°, preferably closer than 1°. From Chapter 29. in [1] the isoplanatic patch size is given as 3-4° at 4 m wavelength. If the calibrator is within a 1-2 degrees from the target, it is possible to use a single beam and then use the *shift+average* procedure, described in Sect. 1.1.3, to produce two datasets, one for the target and one for the calibrator.

Finding a strong, compact (or a subarcsecond resolution modelled) calibrator within 1° is challenging, mainly because the sky is largely unknown at LOFAR frequencies. Efforts are under way to build catalogues of suitable sources at LOFAR frequencies, but often a good first guess can be found by looking at the VLBI catalogue at higher frequencies: http://astrogeo.org/calib/search.html. Often one have to settle for a calibrator which is compact and near the target but which is not bright enough to calibrate the phase and amplitude separately for each visibility (i.e. each channel/integration time). The obvious solution to increase the signal-to-noise (SNR) is to average the data. For shorter baselines, one may usually average several channels and time bins together, provided that the errors because of e.g. the atmosphere does not introduce phase or amplitude changes within the averaging interval. However, for long baselines the errors are more serious, for example because of the very different atmospheres above the stations. The ionosphere may introduce *delay* errors (phase slope vs. frequency) of several hundred nanoseconds, which means that the visibility phases will change several cycles within a few MHz of LOFAR data. Blindly averaging such data will severely reduce the amplitude of the calibrator signal. If the phase also changes with time there will be a phase slope vs. time as well, which is referred to as a fringe *rate*. This means that simple averaging cannot be done to increase the SNR. This is usually the case also in cm-VLBI, and to be able to use the weaker calibrators the VLBI community has developed a technique usually referred to as *fringe fitting*.

1.1.5 Fringe fitting

The precedure used to find and correct residual rates and delays is called *fringe fitting*. A fringe fit is nothing more than a self-calibration including not only phases and amplitudes, but also derivatives of the phase with respect to frequency and time. By doing this, more data can be included in the fitting process thereby increasing the signal-to-noise, which enables solutions to be found for weak sources and/or in noisy data. Fringe fitting is described on example LOFAR data in Sect. 1.2.6. For a more extensive theoretical background, see [1] Chapter 22 and references theirin, in particular [4].

1.1.6 Distributing bandwidth on calibrators

In the M82 observations, we spent equal bandwidth on target and calibrator. This is in principle not necessary, since the calibrator is bright we can use fewer subbands on the calibrator and thereby get more subbands i.e. lower continuum noise on the target beam. To use fringe finding, we need to sample accurately the residual delay/rate slope (and possibly curvature at low frequencies) present in the data. This can be done with sparse sampling in frequency, where the optimal coverage is achieved by spreading the subbands as a powerlaw density with denser placement of subbands at lower frequencies. The advantage of this approach is that more bandwidth can be placed on the target. The disadvantage is that the calibration becomes a bit more demanding. One reason for this is that the UVFITS format used by AIPS (for running fringe fitting) requires data in all channels. If we do not have contigouse subband coverage in frequency, we need to insert fake data and flag that (e.g. using NDPPP, see Sect. 1.2.2) before reading the data into AIPS. This will cause an increase in data volume which will slow down processing. Also, spreading the subbands sparsely is always a risk in case your calibrator is weaker than you think. If you want to use the sparse sampling of subbands, we reccommend you take a look at the paper en titled "Optimum estimate of delays and dispersive effects in low-frequency interferometric observations" (http://dx.doi.org/10.1051/0004-6361/200913951) from 2010. This paper analyses on how to distribute subbands specifically in LOFAR observations for optimal fringe detection.

1.2 Calibration example step by step: The M82 data

In this section we will take a look at a practical example: the M82 dataset published by [2]. These data were taken in project LC0_026 and observed in two parts to maximise hour angle coverage during night time: 10 hours taken during the night between the 20th and 21st of March 2013 and 6 hours taken in the evening of April 5th 2013. Both the March and April observations included the same 44 LOFAR high band antenna (HBA) stations: 23 core stations (CS), 13 remote stations (RS), and eight international (INT) stations. Participating INT stations were DE601, DE602, DE603, DE604, DE605, FR606, SE607, UK608.

1.2.1 Plan of the observations

The observations were designed to image the galaxy M82 with long baselines. Although M82 is bright (>10 Jy) at NL-resolution, it is weak and complex with many compact objects at subarcsecond resolution. This means M82 cannot be used as calibrator itself, and another nearby object was needed. At international baseline resolution, the nearby galaxy M81 is dominated by its AGN, M81*, which is compact, and we chose to include M81, 0.5 degrees from M82, as a nearby phase calibrator. However, M81*

is known to vary in brightness between about 50-150 mJy and we did not know if it would be strong enough to use as calibrator, even with fringe finding to lower the SNR threshold required. Since these were one of the first long baseline science observations, we wanted to be safe and included also an extra calibrator which was compact and brighter. We chose J0958+6533, about 4 degrees from M82, which we found using the VLBI calibrator search tool available here: http://astrogeo.org/calib/search.html. The large angular separation is not optimal, and we cannot expect the phase corrections to be valid across 4 degress. However, a major part of the corrections will be the same, so if by finding corrections for the amosphere on J0958+6533, we should be able to calibrate M81* well enough to see a clear signal, and then we can improve the corrections further by calibrating using M81* itself before finally transferring the calibration corrections to M82. This is a two-step phase-referencing process, where we use two calibrators to find good and better corrections before imaging the target.

Dividing the bandwidth

We aimed to observe at two continuum bands, at 118 Mhz and at 154 MHz. Unfortunately the shift+average approach (sect. 1.1.3) was not available when these observations were performed, and therefore we had to divide the available bandwidth in three separate beams, one on M82, one on M81* and one on J0958+6533. Today, we would still need a separate beam on J0958+6533 since it is far outside the station beam, but we could obtain the M81* and M82 data from the same beam using the shift+average procedure. Since we divided the total bandwidth of 96 MHz (with 200MHz clock at HBA) at two continuum bands for three objects, we ended up with 16 MHz bandwidth for M82 at 154 MHz.

Flux calibration

From the VLBI calibrator catalogue we know that also J0958+6533 may vary in flux density over time. If we had known the flux density of this object at our observing frequency, we chould have used it at flux calibrator directly. However, we now needed to include a final extra calibrator to fix the absolute flux scale. We chose to include 3C196, which is very bright and well known (approx 90 Jy, HEALDREF). Since it is so bright, we only need a few minutes of data and we chose to observe this source for two minutes once every hours. These observations also served to make it possible to *phase up the core* if it had been necessary for fringe finding, see Sect. 1.2.12.

Observational summary

So, to sum up: The plan was to observe 3C196 for two minutes every hour, and the rest of the time divide the bandwidth in three beams, placed on M82 (the target) M81 (nearby but weak calibrator) and J0958+6533 (stronger calibrator further away). No demixing was necessary, so the pipeline requested after observation was just standard flagging, and then averaging to 2s, 4ch/SB before storing in the archive. We wanted to be safe from large residual delays etc.

The first step we want to do to calibrate the M82 data is to find delay and rate corrections (fringe finding) using the source J0958. However before wants we have a few needs, and I will describe these in detail below. First we need to get the data!

1.2.2 Get the data into single MS

The first thing to do is to get the data. The data was put in the LOFAR long term archive (LTA) as a lot of separate files. First one needs to download all the relevant files from the archive. This takes a while, since the data were stored in 2s, 4ch/SB resolution. In the LTA the data were stored as one file per subband per hour, so for the upper 16 MHz data for J0958+6533 I had to download and keep track of 81 * 16 = 1296 files for this source. The split per hour was done since we interrupted the observations once every hour with a 2 minute scan of 3C196. After checking the cookbook and talking with science support, I converged on the following procedure: First combine all subbands together within each 1h block giving 16 MS files, then combine those together to a single MS.

I started trying to combine all subbands, but unfortunately, not all files were present because of a few random failing nodes in the observatory pipeline. Since a few missing subbands is not important here, I used NDPPP to insert fake data (completely flagged) where the missing subbands were. Example parset for combining all subbands for the same 1h block:

```
msin = [..., 'L118547_SB441_uv.dppp.MS', 'SB442_MISSING',
        'L118547_SB443_uv.dppp.MS', ...]
msin.missingdata=True
msin.orderms=False
msin.datacolumn = DATA
msout = J0958_L118547_154MHZ_HOUR1.MS
```

The list of input ms has to be ordered correctly in frequency, then the missingdata flag will fill any non-existent file with fake data (in this case SB442). At this point we also averaged the data to 10s, 1ch/SB to speed up the calibration process. This was done by adding the following lines to the NDPPP parset:

```
averager.freqstep = 4
averager.minperc=0.0
averager.minpoints=0
averager.timestep=5
averager.type=averager
steps = [averager]
```

(Note that the data were previously averaged to 4ch/SB and 2s by the pipeline).

After running the parset we had 16 MS files for source J0958 at 154MHz, one for each of the 16 hours. These were now combined using the task *concat* in CASA:

```
concat(vis=['HOUR1.MS', 'HOUR2.MS', ...], concatvis = 'OUT.MS')
```

For convenience: changing source names

In subsequent tasks you will often have to specify a source name. By default, the LOFAR MS will have source names called `BEAM_0` or similar. It is often hard to remember which source had what beam-index, and therefore it may be useful to change the source names to something more useful. This can be done interactively using the task *browsetable* in CASA. After opening the task, open the MS, press 'Table keywords' on the left, double click on the row 'FIELD', and then double click on the source 'NAME' column. If you get a warning that the browser is not in editor mode, you may enter edit mode by pressing CTRL+E, or use the 'Edit menu' and press 'Edit table'. When you have changed the source name, close the MS to save the changes.

1.2.3 Converting from linearly polarised MS to circularly polarised UVFITS

Global fringe fitting solving for delays and rates is, when writing this, only available within the Astronomical Image Processing System (AIPS, see http://www.aips.nrao.edu). To read the data into AIPS, we first need to convert from the standard LOFAR format of Measurement sets in alinear (X,Y) polarisation basis to UVFITS-files in a circular (R,L) polarisation basis. This is done in two steps, first the conversion to circular and then the conversion to UVFITS.

Conversion to circular polarisation basis

Standard VLBI techniques like fringe fitting work in a circular (R,L) polarisation basis. In this basis, the ionospheric disturbances are transformed from coupled amplitude/phase effects (as in the linear X,Y basis) to phase only effects. Also, since differential Faraday rotation does not mix R and L polarisations we may calibrate RR and LL independently. Conversion to circular polarisation may be done using different tools. The M82 data [2] were converted from linear to circular using the tool *mscorpol* v1.6, developed by T. D. Carozzi. This tool includes corrections for dipole-projection effects as a function of the correlated sky position relative to all included LOFAR stations. After the conversion, the data are circularly polarised, with full (but approximated) parallactic angle correction. Normally the script is executed on an MS file to produce dipole corrected data in a circular basis. The shell command:

```
mscorpol -f INPUTFILE.MS
```

produces corrected data in the DATA column. For more info see the mscorpol manual.

The UV-FITS format

Since AIPS understands the UVFITS-format, but not Measurement Sets (MS) we need to convert the data from MS to UVFITS. There are several ways to do this:

- You may use the function *exportuvfits* in CASA.
- You may use the tool *ms2uvfits* available at the LOFAR cluster, as `ms2uvfits in=[input-MS] out=[output-FITS-file] writesyscal=False`

Note that in a UVFITS file there MUST be data for all baselines included, although data can be flagged if baselines are bad. If one tries to reduce data size by exluding particular subarrays with NDPPP one may run into very strange errors in AIPS, since the basic assumptions of UVFITS are not valid. Hence, it is important to ensure that data are contigous in frequency (e.g. by inserting fake data as explained above) and that there are data present for all baselines in the dataset.

1.2.4 Loading the data into AIPS

The AIPS task FITLD can be used to load the data in to AIPS. For LOFAR data, the parameters digicor=-1 and douvcomp=-1 should be used.

1.2.5 Introduction to AIPS tables

In AIPS one calibrates data by sucessively finding and improving corrections for the amplitude and phase of visibilites. These corrections are stored in tables. Each correction derived is store in an 'SN'

table, and the cumulative corrections are stored in a 'CL' table. The SN table will have a resolution which you specify for each task, i.e. if you find corrections averaging data in two minute chunks, the SN table will have one value every two minutes. The CL table may have a different granularity, so that when applying a specific SN table, you may (automatically) interpolate to CL-table entries between the SN entries. When you are done with calibration, the CL-table including all your corrections can be multiplied with your data using the task SPLIT to produce a UVFITS file with the corrected data.

In this example we will produce SN tables with the tasks FRING (to find delay/rate corrections) and CALIB (to find amplitude/phase corrections). These SN tables are applied to the data by successive application of the specific SN table to the latest CL-table, thereby creating one single CL table containg all corrections.

1.2.6 Fringe fitting

In AIPS the most commonly used task for this is called `FRING`. This task considers the first derivatives of phase vs. frequency and time, i.e. it assumes linear delays and rates within the selected bandwidth and solution interval. As an example, let's inspect two minutes of data on a particular baseline (CS001HBA - DE601HBA) for the source J0958+6533, the source used to find and correct residual delays and rates by [2]. The raw-data is plotted using the AIPS task `POSSM` in Fig. 1.1(a). From this figure we can see by eye that the phase ϕ changes approximately $\Delta\phi = 1.5$ cycles (i.e. $1.5 \cdot 2\pi$ radians) over the full bandwidth of $\Delta\nu$ =15.9 MHz. Assuming a linear phase gradient we can estimate the delay as $\tau = \Delta\phi/\Delta\nu = 94$ ns at this particular time. Indeed, FRING finds a very similar value as can be seen around 22 UT in 1.2(a). These corrections were found using the default parameters of FRING, with the following manual changes: The search was restricted to baselines longer than 60kλ (`uvrange = 60,0`), a delay search window of 600 ns (`dparm[2]=600`), a rate search window of 30 mHz (`dparm[3]=30`), and a solution interval of 2 minutes (`solint=2`). Solutions were found separately for each IF and polarisation. A ParselTongue code snippet (see Sect. 1.2.10) doing this is:

```
fring=task('fring')
fring.indata = data
fring.docalib = 1 # Use any previous calibration,
                  # not relevant since this is first
                  # cal step, but in case one derives
                  # other corrections before, this need
                  # to be included
fring.gainuse = 0 # Use highest CL version
fring.calsour = [None, 'J0958']
fring.refant = 1 # Reference antenna.
fring.snver = 1 # The output SN table version
fring.solint = 2.0
fring.dparm[2] = 600 # ns delay window
fring.dparm[3] = 30 # mHz, for speed
fring.uvrange = [None, 60, 0] # use only long baselines
fring.go()
```

Inspect the solutions carefully with SNPLT after use of FRING. The solutions should be smoothly varying with time, and are typically a few tens of nanoseconds for most antennas. Large delays (microseconds or above) should be reported to the Observatory, particularly if they appear in more than one dataset or if there are sudden changes in the delay.

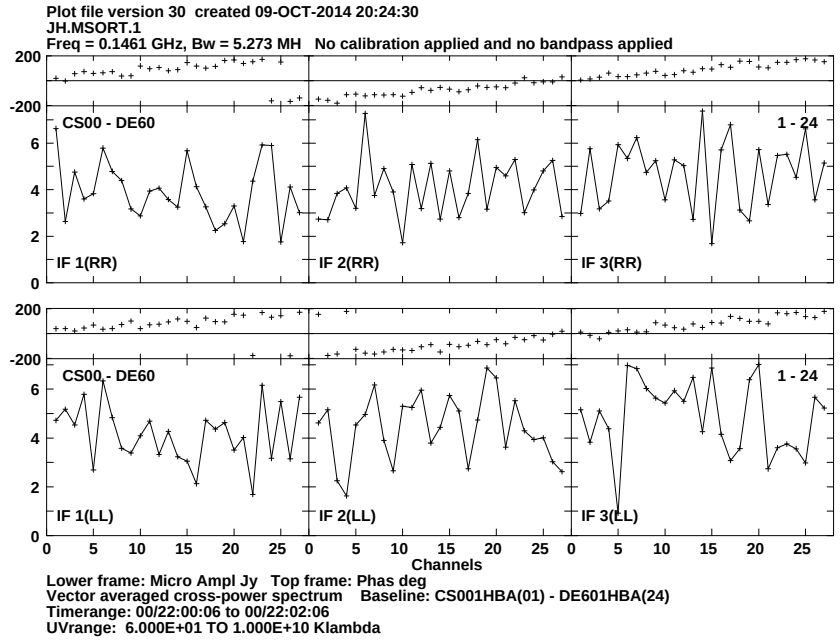

(a) Before fringe fitting

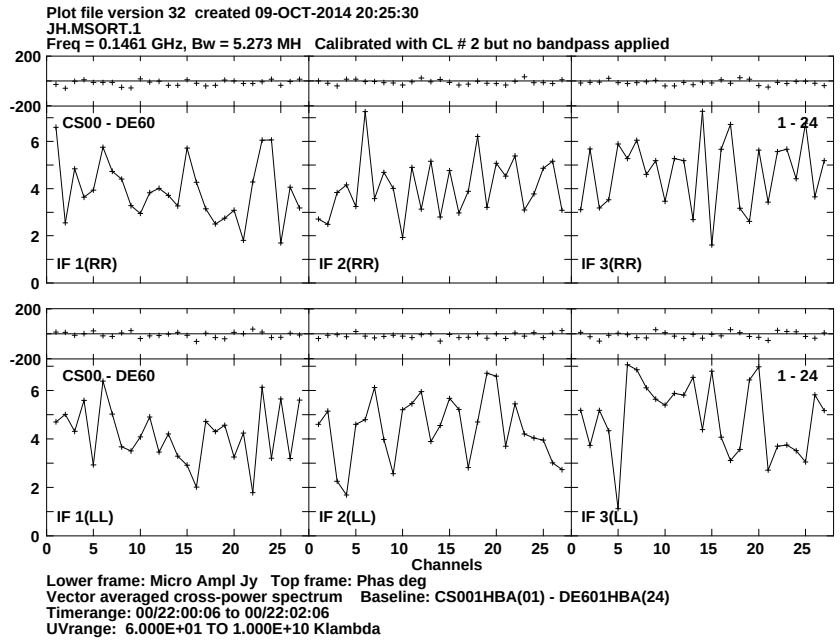

(b) After fringe fitting

Figure 1.1: Two figures showing the effect of fringe fitting on two minutes of data on the baseline CS001HBA - DE601HBA. Both polarisations are shown, and the data are divided in three spectral windows (IFs in AIPS) of 5.3 MHz each. After applying the corrections from FRING, the phase is flat with respect to frequency, see (b), as it should be for a point source.

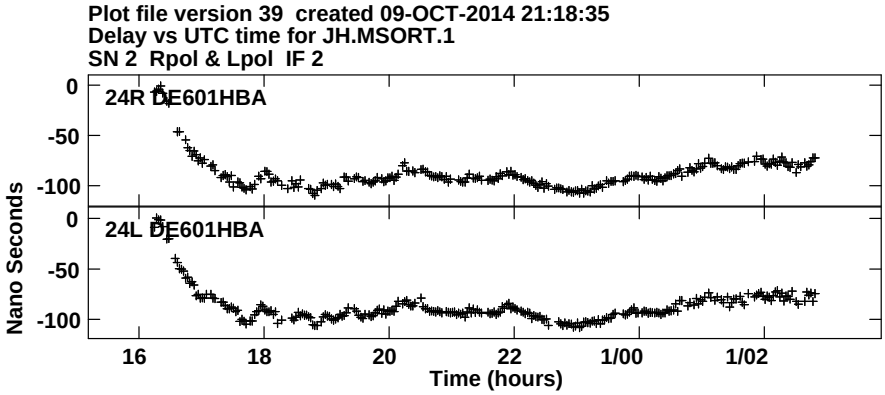

(a) Delay corrections for DE601HBA IF2

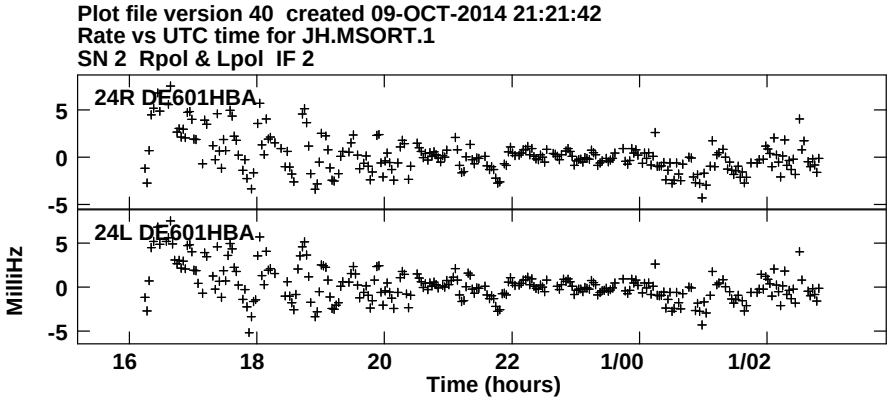

(b) Rate corrections for DE601HBA IF2

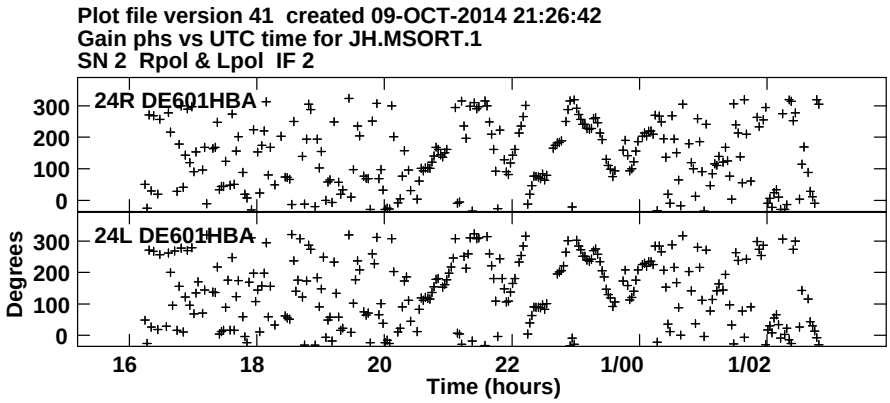

(c) Phase corrections for DE601HBA IF2

Figure 1.2: Delay ((a)), rate ((b)) and phase (c) corrections derived for the source J0958 at 154 MHz by FRING for antenna DE601HBA. These plots show the corrections derived for the whole 10 hour observation (the first segment of project LC0_026). It is clear from the rates and phases that phases changes rapidly during the first and last hours of the experiment. The delay solutions are more stable, although there is a large change in at the start. In general, the ionosphere is more stable during midnight than at sunset or sunrise.

1.2.7 Smoothing/filtering the solutions

Sometimes it is desirable to smooth the solutions if they are very noisy, or to use a median window filter to remove obvious outliers. This can be done with the task SNSMO. Note however that smoothing the solutions can be very dangerous, care needs to be taken when doing this to ensure you do not change the solutions in a way to lock in subtle errors which may affect your calibration later. To remove obivious outliers in the FRING solutions, the following input to SNSMO was used (given in ParselTongue format, see Sect. 1.2.10) to smooth the FRING solutions (SN1) for the J0958 calibration:

```
data = UV(NAME, CLASS, DISK, SEQ)
snsmo = task('snsmo')
snsmo.default()
snsmo.indata = data
snsmo.samptype = 'MWF'
# Support times for filter, in hours
snsmo.cparm[2] =  0 # phase
snsmo.cparm[3] =  0.3 # rates
snsmo.cparm[4] =  1.0 # singleband delay
snsmo.cparm[5] =  1.0 # multiband delay
# Clip thresholds
snsmo.cparm[7] =  400 # maxphas, degrees, i.e. no clip based on phase
snsmo.cparm[8] =  10# max rates, mHz
snsmo.cparm[9] =  100 # max single delay, ns
snsmo.cparm[10] =  100 # max multi delay, ns
snsmo.inver = 1 # The SN table to be smoothed
snsmo.outver = 2 # The SN table where to put new solutions.
snsmo.smotype = 'VLBI'
snsmo.refant = 1
snsmo.doblank = -1
snsmo.go()
```

This produced SN version 2, which is in fact what is shown in Fig, **??**. In this case only a few points were removed and the original version 1 was very similar to after filtering.

1.2.8 Applying the solutions with CLCAL

Now we have derived (and filtered outliers) delay/rate/phase corrections for J0958, and saved these in SN table version 2. These solutions now need to be applied to the data, usint the task CLCAL. An eample ParselTongue code snippet to do this:

```
clcal = task('clcal')
clcal.default()
clcal.indata = data
clcal.snver = 2 # The SN table to apply
clcal.invers = 2 # Again, the SN table to apply. Two lines, since
                 # CLCAL can apply a range of tables (not used here).
clcal.calsour = [None, 'J0958'] # None needed in ParselTongue syntax,
                                # since AIPS counts from 1, and python from 0.
```

```
clcal.gainver = 1 # Old CL version, containing all corrections before FRING
clcal.gainuse = 2 # New CL table version including also FRING corrections
clcal.refant = 1
clcal.go()
```

After applying the corrections from FRING, the phase is flat with respect to frequency, see 1.1(b), as it should be for a point source.

1.2.9 Amplitude calibration: bootstrapping to short baselines

As described earlier the calibrator used for deriving delay, rate and phase corrections need to be close to the target and sufficiently compact to show enough signal on the longest baselines. This calibrator can in principle also be used for amplitude calibration of the long baselines, but again a good model is required. For fringe finding, the only requirement for good solutions is that the calibrator is bright enough and compact enough. But, for amplitude calibration, we must know the flux density of the calibrator. Usually the VLBI calibrators stay compact, but the flux density can vary more than a factor of two between observations due to intrinsic variability. Therefore they cannot be trusted to set the amplitude scale of the observation.

For the case of M82, the calibrator J0958 is bright and compact enough for amplitude calibration of the international baselines, but we did not know the correct flux density. Therefore, we included observations also of a known flux calibrator, 3C196. Now, the calibrator J0958 was used to track possible amplitude variations during the observation for all stations, and 3C196 was used to check the absolute amplitude scale, i.e. to find the flux density of J0958.

The amplitude corrections should be smooth, and will in most cases show a larger gain at the start and end of an experiment. This is because an observation is usually centered in time so that the target will reach its peak elevation at the middle of the observation time. This means that it will be at lower elevation in the begining and end of the observation, which means that the projected station area will be less at the start and end times. This in turn means that the sensitivity is lower at the start and end times, which means that the gain corrections need to be larger (and will be noisier) at these times. As an example, let us look at the gain corrections derived by CALIB in AIPS for DE601HBA on J0958, see Fig. 1.3. When running CALIB, we have decreased the number of free parameters compared to FRING, since we are now only solving for amplitude and phase. It is therefore possible to find minor phase corrections at this point which was not perfectly determined by FRING.

The final result of calibration for this baseline can be seen in Fig. 1.4.

These solutions were now transferred to 3C196, which was imaged using NL-baselines only to check the flux scale. More details by [2].

1.2.10 ParselTongue - Scripting AIPS with python

TODO: Brief section with examples and ref on ParselTongue scripting. In practice, I rarely use pure AIPS nowadays, almost all through ParselTongue / Eskil

1.2.11 High-resolution imaging

Although AIPS can determine delays and rates, it is not the best option for imaging long baseline LOFAR data. Since we consider asmall field of view, we do not need the beam models offered by AW-imager. However, at subarcsecond resolution we will may need to take into account any effects of

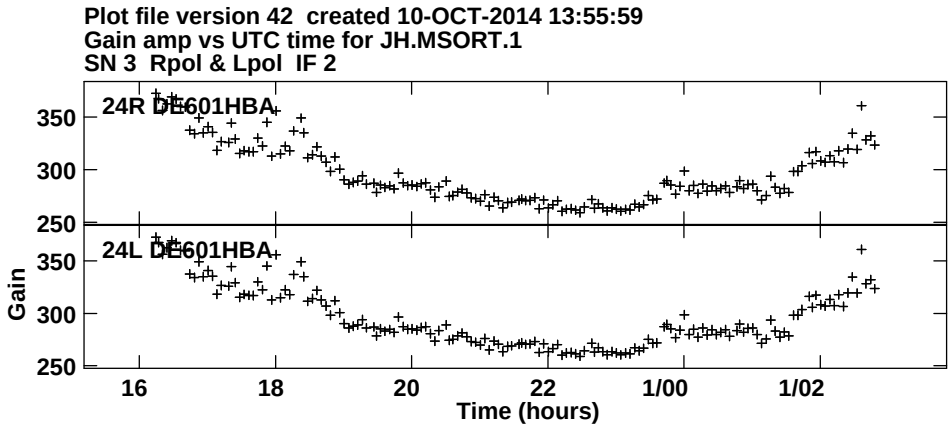

(a) Amplitude corrections for DE601HBA IF2

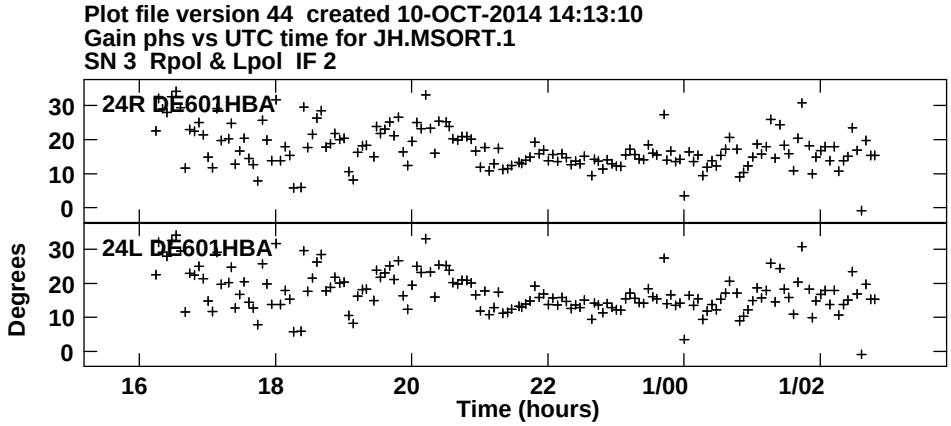

(b) Phase corrections for DE601HBA IF2

Figure 1.3: The amplitude and phase corrections derived by CALIB for the international LOFAR station DE601HBA during the first 10 hours of project LC0_026. We see larger, and more noisy, corrections at the beginning and end of the experiment, as expected from the smaller projected station area at these times relative to transit.

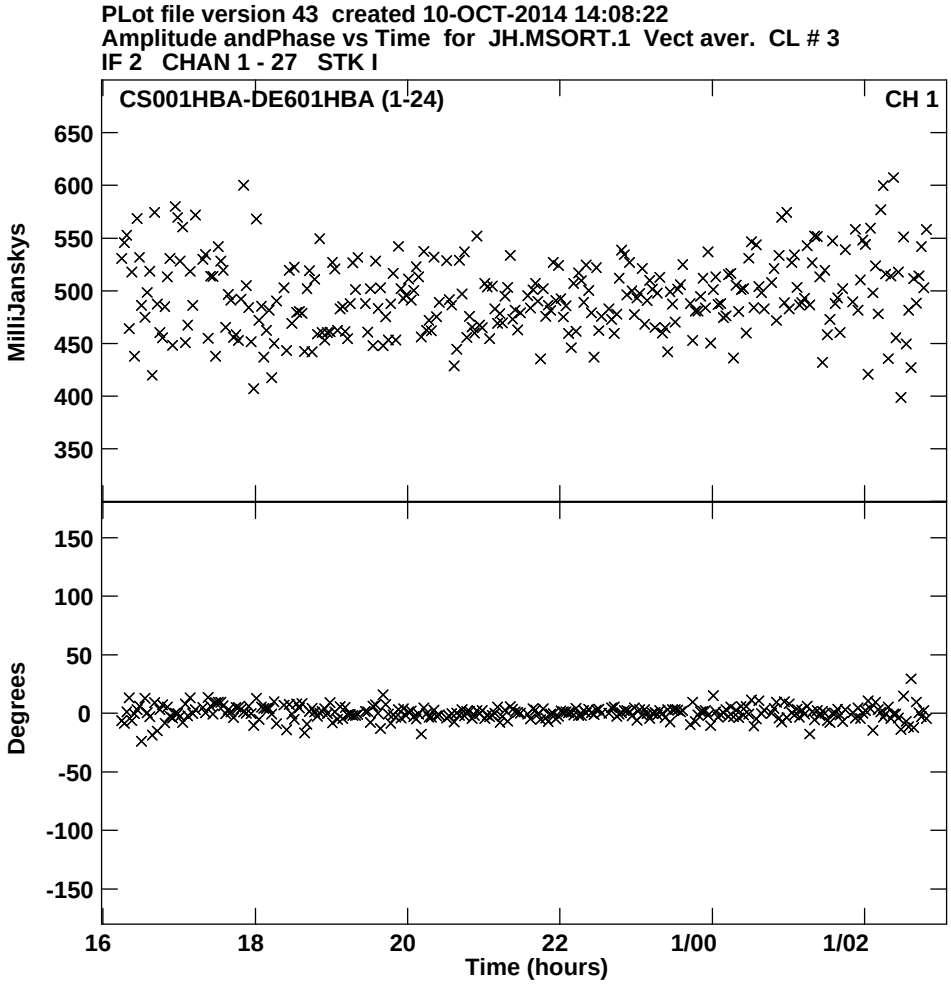

Figure 1.4: The final visibility amplitudes and phases on the DE601HBA-core baseline. We assumed this source to be a 0.5Jy point source, which means that we should now see two straight lines in this plot: one for the amplitude centered at 500 mJy, and one for the phase centered at 0 degrees. This is also what we see using VPLOT in AIPS to inspect the data. Apart from noise, there are marginal changes differences to a point source. It is clear from [2] that this object has a weak extension to the south-west, and this should create minor deviations in the visibilites compared to those of a point source.

a non-coplanar array, i.e. W-projection. The field of view θ_f possible to image without W-projection (i.e. using a single tangent plane) can be estimated as $\theta_\mathrm{f} = \sqrt{\theta_\mathrm{b}}/3$ (see 2-29 in [1]) where θ_b is the FWHM of the synthesized beam, both θ in radians. This expression assumes that we may tolerate phase errors from no-coplanar effects of up to 0.1 radians in our image. If your field to image is larger than this you need to perform deconvolution using W-projection, for example in CASA.

1.2.12 Combining the core into a single superstation

TODO: This section chould include parset files, background info about strong calibrator and also plot of the station beam producet by the phased up core. Eskil's calculations at 154MHz suggest 5% amplitude loss at $30''$ distance from phase center, which is the most serious of all effects mentioned in this document regarding field of view. Also, it is not clear to me if NDPPP phase-rotates the data properly when adding the beams in a specific direction, if using the shift-average approach in the coming pipeline.

1.3 Scheduling long baseline LOFAR observations

TODO: Maybe good to summarise how to select calibrators, subbands etc.?

Bibliography

[1] Taylor, G. B. and Carilli, C. L. and Perley, R. A.*Synthesis Imaging in Radio Astronomy II*, ASPCS 180, 1999.

[2] E. Varenius et al, *Subarcsecond international LOFAR radio images of the M82 nucleus at 118 MHz and 154 MHz*, submitted to A&A.

[3] van Haarlem, M. P. et. al. *LOFAR: The LOw-Frequency ARray*, A&A 556A, 2V 2013

[4] Thompson, A. R., Moran, J. M., & Swenson, G. W. 2001, Interferometry and Synthesis in Radio Astronomy; 2nd ed. (Weinheim: Wiley-VCH)